Modelling evapotranspiration in a spring wheat from thermal radiometry: Crop coefficients and E/T partitioning

J.M. Sánchez[1], R. López-Urrea[2], C. Doña[3], V. Caselles[3], J. González-Piqueras[4], R. Niclòs[3]

[1]Applied Physics Department, School of Mining and Industrial Engineering, University of Castilla-La Mancha, Plz. Manuel Meca, 1 13400 Almadén, Spain.

[2]Instituto Técnico Agronómico Provincial de Albacete and FUNDESCAM, Polígono Industrial Campollano, Avda. 2ª-42 B, 02007 Albacete, Spain.

[3]Earth Physics and Thermodynamics Department, Faculty of Physics, University of Valencia, C/ Dr. Moliner, 50 46100 Burjassot, Spain.

[4]Applied Physics Department, School of Agronomic Engineering and IDR, University of Castilla-La Mancha, Av. España s/n, 02071 Albacete, Spain.

Correspondence to: J. M. Sánchez (juanmanuel.sanchez@uclm.es),

Phone: +34 659092160

Abstract

Wheat is one of the crops occupying the largest areas in the world (218 million ha in 2013). Understanding the land-atmosphere energy exchanges over these croplands becomes important not only for agronomy but also for climatic and meteorological aspects.

This study continues previous work on the estimation of actual evapotranspiration and the assessment of crop coefficients of sorghum, sunflower, or canola. Two variations of a simple two-source energy balance (STSEB) approach were used in combination with land surface temperature measurements to calculate hourly and daily values of surface fluxes and actual evapotranspiration (ET). An experiment was carried out during the spring season of 2014 in Las Tiesas experimental farm in Barrax, Spain. Soil and canopy temperature components together with meteorological variables and biophysical parameters were measured from planting to senescence. Comparison to lysimeter measurements showed calculation errors of ±0.11 mm h^{-1} and ±0.8 mm d^{-1} for hourly and daily ET values, respectively, whereas an underestimation no greater than 4% resulted from the entire campaign. Partition between soil and canopy components yielded a ratio of evaporation (E) to transpiration (T) of 36% to 64%, respectively, for the total growing season. Dual crop coefficients were also calculated and compared to those proposed by FAO56.

Although separate E and T measurements were not available, similar results between the STSEB and FAO 56 models demonstrate the utility of the STSEB for investigating management strategies aimed at increasing crop water use efficiency.

Keywords: Radiometric temperature, evapotranspiration, crop coefficient, two-source energy balance, spring wheat.

1 Introduction

Better management of water resources becomes critical for sustainable development as a consequence of increasing global water demand and severity of droughts. Nowadays, crop irrigation remains the main source of water consumption. This work focuses on

wheat, which is one of the most important crops worldwide, covering a total area of 218 million ha in 2013. In the European Union (EU) more than 25 million ha were cultivated in the year 2013 with a production of 143.3 million tons, approximately 20% of world production. Spain is the fifth producing country within the EU, with an area of 2.1 million ha and a production of 7.6 million tons (FAO 2014). Wheat area in Spain has increased almost 20% in the past 4 years. Castilla y León is the Spanish region with the largest surface area of wheat (around 780,000 ha), while Castilla- La Mancha holds second place with nearly 320,000 ha (MAGRAMA 2014). In this framework, understanding the land-atmosphere energy exchanges over wheat crop becomes important not only for agronomy but also for climatic and meteorological aspects.

The most common approach widely used for calculating the soil water balance and estimating crop water requirement is the FAO-56 method (Allen et al. 1998). According to FAO-56, crop actual evapotranspiration (ET) is estimated by the combination of a reference evapotranspiration (ET_o) and crop coefficients. There are two different FAO-56 approaches: single and dual crop coefficients. The single crop coefficient approach is used to express both plant transpiration and soil evaporation combined into a single crop coefficient (K_c). The dual crop coefficient approach uses two coefficients to separate the respective contribution of plant transpiration (K_{cb}) and soil evaporation (K_e), each by individual values (Allen et al. 1998). This dual crop coefficient technique can improve the accuracy of ET estimation although it requires calibration of the coefficients. This technique has been widely applied and explored under a variety of climatic conditions worldwide (Hunsaker et al. 2005;Williams and Ayars 2005; López-Urrea et al. 2009, 2102, 2014; Campos et al. 2010; Howell et al. 2012; Zhang et al. 2013; Ghamarnia et al. 2014). All these authors agree that crop coefficient values taken from literature may serve as a starting point for irrigation scheduling, but corrections to these initial values

become necessary to adjust to local conditions since considerable errors may occur due to their empirical nature. With this aim, many authors have shown the possibility of using remote sensing measurements to estimate crop water requirements and then improve irrigation scheduling and water productivity. Focusing on wheat, López-Urrea et al. (2009) determined crop coefficient of this crop in the semi-arid climatic conditions of Central Spain, using a weighing lysimeter. These authors showed good agreement with the values proposed by FAO-56 and published by other authors. Gontia and Tiwari (2010) generated monthly crop coefficient maps of wheat croplands in India from vegetation indexes information, and used those to estimate ET maps. Zhao et al. (2013) adopted the dual crop coefficient approach to simulate the soil water balance in winter wheat in the North China Plain (NCP), and tested the SIMDualKc model. Gao et al. (2014) calibrated this model in the same Chinese region with data from a winter wheat but with subsurface drip irrigation. Shahrokhnia and Sepaskhah (2013) used weighing lysimeters to evaluate and calibrate the values proposed by FAO for the daily crop coefficient and ET of wheat in the Fars province, Iran. Yang et al. (2014) used a complementary relationship model coupled with an Evaporative Fraction (EF) approach to estimate ET of winter wheat in the NCP, based on meteorological data and a high resolution IKONOS image. Farg et al. (2012) estimated crop coefficients for wheat in the south Nile Delta of Egypt using vegetation indices derived from SPOT-4 satellite data. Zhang et al. (2015) used MODIS data with an energy-balance ET model (EBEM) to estimate daily evapotranspiration in the NCP, and the results were compared to lysimeter measurements.

The combination of two-source energy balance with local radiometric temperatures has been shown to effectively estimate actual evapotranspiration values under a variety of crops and environmental conditions (French et al. 2007; Sánchez et al. 2008, 2011;

Colaizzi et al. 2012; Kustas et al. 2012). The main limitation to the operational application of this technique at a regional scale is the retrieval of land surface temperature from satellite data with the sufficient spatial and temporal resolutions; especially in those agricultural areas composed of cropped fields smaller than 1 ha. Nowadays none of the operating satellites offer the combination of spatial and temporal resolution of thermal infrared (TIR) bands needed for these applications. However, significant progress is being made in disaggregation techniques for downscaling information of TIR bands using higher resolution visible/near infrared (VIS/NIR) bands (Agam et al. 2007; Bindhu et al. 2013; Gao et al. 2012). This is expected to bring the opportunity to use some operating satellites such as SPOT, DEIMOS, or FORMOSAT, and others coming soon, such as the promising SENTINEL-2, which do not include TIR bands but will offer high resolution VIS/NIR images (10-20 m). In a recent paper, Sánchez et al. (2014) applied this technique to separate evaporation (E) and transpiration (T) components and those were used to predict dual crop coefficients for sunflower and canola crops. A new experiment was carried out in the spring growing season of 2014 in a wheat field located in a semi-arid region of Central Spain. The methodology and experimental setup were similar to those already described in Sánchez et al. (2014), so the aim of this work is presenting the new results for a wheat crop and reinforcing the potential of thermal infrared measurements as an alternative technique to FAO-56 for the evaluation and partitioning of ET into E and T components. This can be also considered a useful tool for the local adjustment of the FAO-56 crop coefficients.

2. Materials and methods

This experiment was carried out in "Las Tiesas" experimental farm (2º 5´W, 39º 3´N, 695 m a.s.l) located in the semi-arid, Temperate Mediterranean province of Albacete (Central Spain) from February to June 2014. The study site is a 100 m x 100 m field with a weighing lysimeter (2.7 m long, 2.3 m wide and 1.7 m deep) installed in the center of the plot characterized by a resolution of 0.04 mm equivalent water depth. Weighing lysimeters are presently the most accurate method to measure ET (Howell et al., 1995). The soil is classified as *Petrocalcic Calcixerepts*. Average soil depth of the experimental plot is 40 cm, and is limited by the development of a more or less fragmented petrocalcic horizon. Texture is silty-clay-loam, with 13% sand, 49% silt and 38% clay, with a basic pH (8.1). The soil is low in organic matter (1.48%) and nitrogen (0.10%), and has a high content of active limestone (12.5%). For a more comprehensive description of the site and technical features of the lysimeter see López-Urrea et al. (2006) and Sánchez et al. (2011).

Wheat (*Triticum aestivum* L. cv. ´Califa´) was sowed on February 4 in rows 15 cm apart with a seed population of 550 seeds m^{-2} (Fig.1). Measurements started on 12 February (DOY 43) and lasted to 30 June (DOY 181). Efforts were made to keep the crop inside the lysimeter at the same growth rate and plant population as the crop outside to minimize edge effects. The whole plot has a permanent sprinkler irrigation system with sprinklers placed on a grid of 15 m x 12.5 m that provide a precipitation rate of 8.6 mm h^{-1}. During the experiment wheat was irrigated, avoiding water stress conditions at anytime. Fractional vegetation cover (P_v), and crop height were measured weekly, and then modeled for the entire experiment, to monitor crop development (Fig. 2). The fractional vegetation cover (P_v) was determined using a supervised classification

150 technique of digital photographic images with the maximum probability algorithm
151 (Calera et al. 2001), in order to assign the current classes of green vegetation and soil in
152 the image, based on the classic methodology for calculating green plant cover
153 developed by Cihlar et al. (1987). Digital photographs acquired weekly over the
154 lysimeter area were always taken at solar noon and vertically from an approximate
155 height of 2 m above ground. Supervised classification of these digital images was later
156 carried out with the help of the ENVI® computer program. Crop height (h) was
157 measured also weekly, in plant samples from three separate areas, as the distance
158 between ground level and the peak of the plant. Best fitting values for both P_v and h
159 data series were used to reproduce their curves for the entire experiment.
160 Three Apogee SI-121 Thermal Infrared Radiometers (IRT) (Apogee Instruments, Logan
161 UT, USA) were used in this experiment. These are broad band thermal instruments (8-
162 14 μm) with an accuracy of ± 0.2 ºC, a 18º field of view, and a valid temperature range
163 from -30 to 65ºC. One was placed at a height of 2 m over the lysimeter spot, looking at
164 the surface with nadir view and measuring the composite target temperature (T_R). A
165 second radiometer was placed at a height of 20 cm directly pointing to the soil between
166 rows (Fig. 1) to measure soil temperature data (T_s). Canopy temperature (T_c) values
167 were inferred from T_R and T_s, using P_v information, as described in Sánchez et al.
168 (2014). This experimental setup avoids limitations in obtaining T_c using IRTs with a
169 near-horizontal view, especially for low values of P_v.
170 All temperatures were corrected for emissivity and atmospheric effects. At this point,
171 downwelling sky radiance was calculated from sky brightness temperature values
172 measured by a third Apogee radiometer pointing at the sky with an angle of 53º. Values
173 of ε_c =0.987±0.005 and ε_s =0.960±0.013 were used for this study (Rubio et al. 2003).

Air temperature (T_a) and relative humidity (H_r) were measured using a HMP50 probe (Vaisala Inc., Helsinki, Finland). Wind speed (u) was measured by an anemometer (model A100R, VectorInstruments Ltd., UK). Solar irradiance (S) (model CM14, Kipp & Zonen Delft, Holland) and incoming long-wave radiance (L_{sky}) (model CG2, Kipp & Zonen Delft, Holland) were also measured. Net radiation (R_n) was measured by a NR-Lite sensor (Kipp & Zonen, Delft, The Netherlands) mounted over the lysimeter spot. Soil moisture (SM) was monitored using a capacitance sensor (10HS ECH_2O, Decagon Devices Inc., Pullman, WA) at 10cm depth. All data were stored every 15 min, using a CR-1000 datalogger (Campbell Scientific Inc., Logan, USA), and averaged at hourly scale. Table 1 lists a summary of the mean values of these variables and parameters for the entire experiment.

In this work a Simplified version of the Two-Source Energy Balance (STSEB) (Sánchez et al. 2008) was applied to estimate total and separate soil and canopy energy fluxes using the radiometric temperatures, biophysical information, and meteorological data as inputs. A summary of the different equations, parameters and methodological procedure of the STSEB model is included in the Appendix. The reader is referred to Sánchez et al. (2008) and (2011) for a more comprehensive description. This approach was conceived to be applied when the radiometric temperatures of both soil and canopy are known, or at least one of them together with the composite temperature T_R. However, application of STSEB is also possible when only T_R is available, upon the inclusion of some assumptions as part of the approach, for example an initial calculation of canopy transpiration using the Priestley-Taylor equation (Priestley and Taylor, 1972). A scheme of this formulation of the STSEB-T_R model is included in the Appendix. A test of this version of the model (STSEB-T_R) was carried out, and results were compared to the pure STSEB approach.

Agreement between modeled and measured values of the surface energy fluxes are analyzed in this paper in terms of the parameters of the linear regression adjustment (slope, intercept and determination coefficient, r^2), the root mean squared error (RMSE), and the mean bias error (MBE) (Willmott 1982).

3 Results and discussion

3.1 Comparison between STSEB and STSEB-T_R

Results of the different terms of the energy balance equation were obtained and averaged at an hourly scale, applying both the original STSEB and the modified STSEB-T_R formulations (see Appendix). Figure 3 shows the comparison between the two version outcomes. Differences between the two formulations are negligible in terms of net radiation (R_n) and soil heat fluxes (G), with RMSE values lower than 5 W m^{-2}. Some discrepancies arise in terms of the sensible heat flux (H), with a RMSE=20 W m^{-2}. This absolute error is maintained in ET estimates. However, the non-water-stressed status of this wheat experiment mask this deviation in ET since H is a minor term compared to R_n under these conditions. Nevertheless, a slight underestimation of ET is observed with the STSEB-T_R approach, more evident for large ET values. These results give confidence to the application of the STSEB-T_R scheme in those scenarios where only the composite target temperature is available and non-water-stressed conditions are prevalent. Further adjustments in the Priestley-Taylor approach would be required under different surface and environmental conditions (Colaizzi et al. 2012).

3.2 Modeled wheat evapotranspiration

224 An accurate estimate of the net radiation is critical for obtaining accurate LE values.
225 Figure 4a shows the comparison between modeled and observed values of R_n. A RMSE
226 value of ±35 Wm^{-2}, corresponding to an average relative error of ±10% was observed
227 for both the original STSEB and the STSEB-T_R calculations. These results are very
228 close to the value of ±7% obtained in Zhang et al. (2015) over wheat. Colaizzi et al.
229 (2012) applied the original TSEB approach, using separate measurements of T_s and T_c,
230 to an irrigated cotton crop and observed a very similar RMSE of ±30Wm^{-2} in the
231 retrieval of R_n. Very good agreement was observed also by these authors when
232 comparing TSEB and a modified TSEB-T_R formulation (Colaizzi et al. 2012), in terms
233 of R_n estimates.
234 Hourly values of ET, ranging between -0.2 and 1.2 mm h^{-1}, were compared to lysimeter
235 measurements (Fig. 4b). Using the original STSEB model, a root mean square error of
236 ±0.11 mm h^{-1} was obtained, and the bias was negligible. Similar RMSE= ±0.11 mm h^{-1},
237 with an underestimation of -0.03 mm h^{-1} and a slightly larger scatter, resulted from the
238 application of the STSEB-T_R approach. These results are an improvement over Sánchez
239 et al. (2011) and (2014), where RMSE values close to ±0.20 mm h^{-1} for sunflower and
240 canola, and ±0.14 mm h^{-1} for sorghum, were observed.
241 The original STSEB approach will be used hereafter for the rest of the analysis since, as
242 shown above, it seems to reproduce slightly better results than the STSEB-T_R in this
243 work.
244 The evolution of the daily ET (ET_d) values, modeled and measured, are shown in Fig.
245 5a. Average ET_d value remained below 3 mm d^{-1} until the end of March, peaked 9-10
246 mm d^{-1} between middle May and middle June and declined afterwards during the grain
247 filling through physiological maturity period. In general, lysimeter ET_d values are well
248 captured by the STSEB model estimates for the entire wheat growing season, except

very few days when some rain events occurred and the lysimeter measure had to be recalculated. Following these precipitation events, and very few other weight and calibration verifications, the lysimeter mass data were interpolated using measurements made immediately prior to and immediately following dates that required adjustments. As shown in Figure 5b, discrepancies were within ±1.0 mm d^{-1} for more than 85% of the dataset.

Quantitative analysis of the comparison between modeled and observed daily ET (ET_d) shows an average underestimation of 0.18 mm d^{-1} with a RMSE value of ±0.8 mm d^{-1}, and a determination coefficient (r^2) of 0.903 (Fig. 6). Results are again in agreement with those obtained in Sánchez et al. (2011) and (2014), where RMSE values of ±1.0 mm d^{-1} were observed for sorghum, sunflower and canola, and very close to the RMSE=±1.1 mm d^{-1} shown by Colaizzi et al. (2012) in irrigated cotton fields also using weighing lysimeters. These authors pointed out an underestimation of the TSEB early in the season and an overestimation later on, when using direct T_s and T_c measurements. Note that these direct T_c and T_s measurements consider the contribution of the entire canopy and soil, respectively, accounting for sunlit and shaded portions, and this proportion varies with time of day and canopy structure. Also, some experimental limitations arise when measuring T_c using IRTs with near-horizontal view for low vegetation cover conditions (Colaizzi et al. 2012), resulting in an overestimation of the canopy temperature that yields a subsequent underestimation of ET. Colaizzi et al. (2012) postulated that overestimates of E could be due to model assumptions and T_s measurements not accounting for the whole interrow portion. Late season ET overestimates were also reported by French et al. (2007) for wheat, and they attributed this to leaf senescence. This behavior in the discrepancies is not observed in Figure 5b. Focusing on wheat, Zhang et al. (2013) compared ET values predicted by their

274 simulation model with those obtained from eddy-covariance measurements. Values of
275 RMSE=±0.6 mm d^{-1} and r^2 of 0.92 were observed by these authors in a winter wheat. A
276 similar error of RMSE=±0.4 mm d^{-1}, was shown by Gao et al. (2014) as a result of the
277 comparison between simulations by the adjusted dual crop coefficients and results
278 applying a water balance method. Yang et al. (2014) estimated daily ET using the
279 evaporative fraction method coupled with the daily net radiation, with an overall
280 estimation error of RMSE=±0.7 mm d^{-1} with a determination coefficient of 0.937. A
281 daily average deviation of ±0.9 mm d^{-1} was obtained by Zhang et al. (2015) when
282 comparing lysimeter measurements with estimations using an energy balance model
283 together with MODIS data. In one of the very few ground-validated, ET studies at fine
284 spatial scale for wheat, French et al. (2007) used airborne image observations as inputs
285 in the TSEB model to calculate ET with accuracy to within ±1.3 mm d^{-1} for the full
286 season, when compared to independent soil water depletion observations.
287 The total seasonal evapotranspiration predicted by the STSEB model (500 mm) was less
288 than 4% lower than that measured in the lysimeter (520 mm) (see Fig. 7). Note that this
289 agreement is particularly good for the initial stage (DOY<90), when bare soil and low
290 vegetation coverage conditions are traditionally a challenge for both energy and water
291 balance models (Colaizzi et al. 2012; Shahrokhnia and Sepaskhah 2013).
292
293 3.3 Evaporation/Transpiration partitioning
294
295 The E and T values calculated with the STSEB model using data from the present study
296 are shown in Fig. 7.. Soil E was clearly dominant for vegetation cover fractions below
297 0.2 (DOY<90). The ratio T/E increased very fast, and T became the major contribution
298 to ET after then. The total seasonal E resulted in 180 mm, with about half of this

amount concentrated before DOY 90. Cumulative T value was 320 mm. This means 36% of the seasonal wheat ET corresponds to soil evaporation. This modeled value is in agreement with former studies relative to wheat. López-Urrea et al. (2009) obtained a seasonal evaporation component amounting to 24% (135 mm) of the total ET. Zhang et al. (2013) observed soil evaporation for winter wheat averaged 28% during the full crop season, whereas it represented near 80% for the initial stage and decreased to 5-6% during the mid-season period. Sun et al. (2006) reported 30 to 35% for non-stressed to mild-stressed winter wheat, and Sadras and Rodriguez (2010) reported 22-34% in Australia. Using micro-lysimeters, Shahrokhnia and Sepaskhah (2013) estimated that soil evaporation was about 30% of the total wheat ET. A lower ratio of 19% was obtained for the seasonal E/ET of a winter wheat with a drip irrigation system (Gao et al. 2014). These findings should prompt further field studies of E and T partitioning for different irrigation systems and management strategies.

3.4 Crop coefficients

Figure 8a plots the curve of K_c calculated as the ratio of the lysimeter measured, and STSEB predictions, with the reference evapotranspiration (ET_o) calculated with the FAO-56 Penman-Monteith equation (Allen et al. 1998). K_c values are presented as 5-day averages to avoid the scatter produced by irrigation events. The average K_c data obtained from lysimeter measurements for each stage were: $K_{c\text{-}ini}$: 0.80, $K_{c\text{-}mid}$: 1.18 and $K_{c\text{-}end}$: 0.41, whereas the average K_c values obtained from STSEB calculations were: $K_{c\text{-}ini}$: 0.82, $K_{c\text{-}mid}$: 1.14 and $K_{c\text{-}end}$: 0.59. López-Urrea et al. (2009) reported similar behavior of K_c in a similar experiment over wheat in the same area using also lysimeter measurements. These authors reported wheat K_c values of $K_{c\text{-}mid}$: 1.20 and $K_{c\text{-}end}$: 0.15.

The K_{c_mid} matched our measurements, whereas that difference in the $K_{c\text{-}end}$ is due to the higher values of evapotranspiration at the end of this growth stage in our measurements, consequence of the relatively high value of P_v=0.23 still present in DOY 180. Other authors obtained K_c values of 0.30-0.45 for $K_{c\text{-}ini}$, of 1.10-1.20 for $K_{c\text{-}mid}$, and $K_{c\text{-}end}$ in the range of 0.25-0.45 (Gontia and Tiwari 2010; Kjaersgaard et al. 2008; Howell et al. 2006; Allen et al. 1998). These $K_{c\text{-}mid}$ data are similar to our averaged $K_{c\text{-}mid}$ and small variations can be due to differences in: the planting date, lengths of growth stages, wheat varieties, cultural practices and climatic conditions. Differences in the $K_{c\text{-}ini}$ and $K_{c\text{-}end}$ can be due to the higher values of evaporation during these two stages in our measurements. Shahrokhnia and Sepashkah (2013) estimated values of 0.77, 1.35, and 0.26 for $K_{c\text{-}ini}$, $K_{c\text{-}mid}$, and $K_{c\text{-}end}$, respectively. Average $K_{c\text{-}ini}$ basically matched our measurements and $K_{c\text{-}end}$ was lower than our estimation, whereas our values of $K_{c\text{-}mid}$ were lower than those reported by these authors. These discrepancies could be due to different wheat variety and climatic conditions as well as to eventual deviations in the reference ET calculations.

As stated by López-Urrea et al. (2009), soil evaporation component (E) can be significant when sprinkler system is used for irrigation or frequent rain events occur. This is the case of our study. Note the high values of $K_{c\text{-}ini}$ observed (Fig. 8a) for the initial stage of the wheat growing, with P_v values lower than 0.2.

Dual crop coefficients K_e and K_{cb} were calculated as the ratios E/ET_o and T/ET_o, respectively. Figure 8b shows the comparison between results obtained and values proposed by FAO-56, all 5-day averaged. Relatively large values of K_e were obtained for establishment and the beginning of development stages due to frequent irrigations while the vegetation cover was low. During reproduction K_{cb} increased rapidly and peaked to 1.10 during the ripening stage. The average K_{cb} data obtained from STSEB

calculations for each stage resulted in: K_{cb_ini}= 0.05, K_{cb_mid}= 1.10 and $K_{cb\text{-}end}$= 0.19. Modeled K_{cb} values were smaller than FAO-56 predictions. In terms of K_e, FAO-56 underestimated modeled values, particularly at the initial growth stage. Note that the K_e coefficient is greatly affected by irrigation strategy, soil type, canopy coverage, and local weather conditions.

Zhang et al. (2013) estimated initial, mid-season and end K_{cb} values for wheat of 0.25, 1.15 and 0.30, respectively. Similar values were obtained by Shahrokhnia and Sepaskhah (2013), ranging between 0.18-0.27, 1.11-1.16, and 0.11-0.14 for initial, mid-, and end-season stages, respectively. Gao et al. (2014) also obtained K_{cb} values ranging 0.22-0.27, 1.02-1.10, and 0.25-0.43, for initial mid-, and end-season stages, respectively, in subsurface drip irrigated wheat. All these reported $K_{cb\text{-}mid}$ and $K_{cb\text{-}end}$ values are in agreement with our estimates, whereas those observed $K_{cb\text{-}ini}$ values from previous studies are clearly larger than our predicted average $K_{cb\text{-}ini}$. Differences at this point are likely due to a higher canopy cover during the initial growth stage in the studies reported in the literature.

4 Conclusions

Results in this paper reinforce the potential of the techniques based on the combination of surface energy balance with radiometric temperatures for irrigation scheduling or water management under a variety of crops and surface conditions.

In this work we focused on a spring wheat crop located in a semiarid region of central Spain. Comparison between model estimates and lysimeter measurements showed a RMSE value of ±0.8 mm d^{-1}, in agreement with previous results using the same technique over sorghum, sunflower or canola. Furthermore, this error is maintained for more than 80% of the 130 days of the experiment duration, and equally for all

374 vegetation cover conditions. Accuracy improves when cumulative ET values are
375 calculated. A deviation no greater than 4% (20 mm) is observed for the prediction of the
376 total 520 mm measured for the full wheat growing season.
377 Partition of ET into E and T components resulted in 36% of the total ET corresponding
378 to the soil evaporation, although most of it was concentrated in the initial phase
379 (P_v<0.4). A proper implementation of the STSEB approach might become a useful tool
380 at this point when facing strategies to increase crop water use efficiency through a
381 feasible monitoring of the soil evaporation/transpiration partitioning.
382 Crop coefficient and dual crop coefficients were also computed. Results are in
383 agreement with those K_c obtained from the lysimeter measurements, and the K_{cb}, and K_e
384 values shown by other authors for wheat. This technique could be used for the local
385 adjustment of the FAO56 K_c values, as an alternative in those fields where weighing
386 lysimeters are not available.
387 The main limitation for the operational application of the energy balance modeling at a
388 crop field scale is the coarse spatial resolution of the thermal data provided by the
389 orbiting satellites. Recent advances in downscaling TIR information from low-medium
390 spatial resolution sensors, using VIS/NIR medium-high spatial resolution sensors, bring
391 the opportunity to the operational application of the technique presented from satellite
392 data. With this aim, a modified STSEB-T_R approach was presented. This version was
393 conceived to be applied using the composite target temperature T_R as the unique
394 radiometric temperature input. Results using this new formulation match those using the
395 original STSEB model, under the conditions of the present study. Further work is
396 required, including evaporation and transpiration measurements under different field
397 and environmental conditions, before extracting any firm conclusion at this point.
398

Acknowledgements

This work was jointly supported by the Spanish Ministry of Economy and Competitiveness (projects CGL2013-46862-C2-1/2-P, CGL2011-30433-C02-02, and AGL2014-54201-C4-4-R, and Dr. Niclòs' "Ramón y Cajal" Research Contract) and Generalitat Valenciana (PROMETEOII/2014/086). The Authors would like to thank the logistic support in the instrumentation maintenance of Laura Martinez and Juan A. de la Vara.

Appendix.

The original formulation of the Simplified Two-Source Energy Balance model (STSEB) (Sánchez et al. 2008) used the measured temperature of both soil (T_s) and canopy (T_c) components to calculate the different terms of the energy balance equation:

$$R_n = H + ET + G \quad \text{(A1)}$$

where R_n is the net radiation flux (W m^{-2}), H is the sensible heat flux (W m^{-2}), ET is the latent heat flux (W m^{-2}), and G is the soil heat flux (W m^{-2}).

According to the STSEB approach, the sum of the soil and canopy contributions (values per unit area of component) to the total sensible heat flux, H_s and H_c, respectively, are weighted by their respective partial areas as follows:

$$H = P_v H_c + (1 - P_v) H_s \quad \text{(A2)}$$

where P_v is the vegetation cover fraction at nadir. In equation (A2), H_s and H_c are expressed as:

$$H_c = \rho C_p \frac{T_c - T_a}{r_a^h} \quad \text{(A3a)}$$

$$H_s = \rho C_p \frac{T_s - T_a}{r_a^a + r_a^s} \quad \text{(A3b)}$$

where ρC_p is the volumetric heat capacity of air (J $K^{-1} m^{-3}$), T_a is the air temperature at a reference height (h), r_a^h is the aerodynamic resistance to heat transfer between the canopy and the reference height at which the atmospheric data are measured (s m^{-1}), r_a^a is the aerodynamic resistance to heat transfer between the point z_{0M}+d (z_{0M}: canopy roughness length for momentum, d: displacement height) and the reference height (s m^{-}

427 [1]), r_a^s is the aerodynamic resistance to heat flow in the boundary layer immediately
428 above the soil surface (s m^{-1}). A summary of the expressions to estimate these
429 resistances can be found in Sánchez et al. (2008). Equations (A3a) and (A3b) are taken
430 from the parallel configuration of the TSEB model (Norman et al., 1995; Li et al.,
431 2005), modified to take into account the distinction between r_a^h and r_a^a (Sánchez et al.
432 2008).
433 The partitioning of the net radiation flux, R_n, between the soil and canopy is proposed as
434 follows:

435 $$R_n = P_v R_{nc} + (1 - P_v) R_{ns} \quad \text{(A4)}$$

436 where R_{nc} and R_{ns} are the contributions (values per unit area of component) of the
437 canopy and soil, respectively, to the total net radiation flux. They are estimated by
438 establishing a balance between the long-wave and the short-wave radiation separately
439 for each component:

440 $$R_{nc} = (1 - \alpha_c) S + \varepsilon_c L_{sky} - \varepsilon_c \sigma T_c^4 \quad \text{(A5a)}$$

441 $$R_{ns} = (1 - \alpha_s) S + \varepsilon_s L_{sky} - \varepsilon_s \sigma T_s^4 \quad \text{(A5b)}$$

442 where S is the solar global radiation (W m^{-2}), α_s and α_c are soil and canopy albedos,
443 respectively, σ is the Stefan-Boltzmann constant, and L_{sky} is the incident long-wave
444 radiation (W m^{-2}).
445 A similar expression is used to combine the soil and canopy contributions, ET_s and ET_c,
446 respectively, to the total latent heat flux:

447 $$ET = P_v ET_c + (1 - P_v) ET_s \quad \text{(A6)}$$

448 According to this framework, a complete and independent energy balance between the
449 atmosphere and each component of the surface is established, from the assumption that
450 all the fluxes act vertically. In this way, the component fluxes to the total latent heat
451 flux can be written as:

452 $$ET_c = R_{nc} - H_c \quad \text{(A7a)}$$

453 $$ET_s = R_{ns} - H_s - \frac{G}{(1 - P_v)} \quad \text{(A7b)}$$

454 Finally, G can be estimated as a fraction (C_G) of the soil contribution to the net radiation
455 (Choudhury et al. 1987):

456 $$G = C_G (1 - P_v) R_{ns} \quad \text{(A8)}$$

457 where C_G can vary in a range of 0.2-0.5 depending on the soil type and moisture. A
458 value of C_G=0.35 was used in this work.

When the composed target temperature (T_R) is the only measurement available, the original formulation of the STSEB needs the inclusion of additional assumptions to calculate, for example, an initial estimate of canopy latent heat flux. In this STSEB-T_R approach, the Priestley-Taylor equation was used:

$$ET_c = f_g \alpha \left[\frac{\Delta}{\Delta+\gamma}\right] R_{nc} \quad \text{(A9)}$$

where f_g is the fraction of the vegetation that is green, Δ is the slope of the water vapour saturation curve, α is the Priestley-Taylor (PT) parameter (Priestley and Taylor, 1972), and γ is the psychrometric constant. A value of α=1.26 was assumed in this study, according to the non-water-stressed conditions over this wheat field (French et al. 2007). Note that this value might need adjustment under water-stressed conditions.

An initial value of T_c is extracted by solving the equation resulting from the combination of (A5a), (A7a), and (A9). Then, the corresponding value of T_s can be calculated from the equation (Sánchez et al. 2008):

$$\varepsilon T_R^4 = P_v \varepsilon_c T_c^4 + (1 - P_v) \varepsilon_s T_s^4 \quad \text{(A10)}$$

where ε_c, and ε_s, are the canopy and soil emissivities, respectively, ε is the effective surface emissivity. Once T_c and T_s values are estimated, equations (A2)-(A8) can be applied.

Conflicts of interest

The authors declare no conflict of interest

References

Agam N, Kustas WP, Anderson MC, Li F, Neale CN (2007) Avegetation index based technique for spatial sharpening of thermal imagery. Remote Sens Environ 107:545-558

Allen RG, Pereira LS, Raes D, Smith M (1998) Crop evapotranspiration: guidelines for computing crop water requirements, in: Proceedings of the FAO Irrigation and Drainage Paper No.56. Roma, Italy

488 Bindhu VM, Narasimhan B, Sudheer KP (2013) Development and verification of a
489 non-linear disaggregation method (NL-DisTrad) to downscale MODIS land
490 surface temperature to the spatial scale of Landsat thermal data to estimate
491 evapotranspiration. Remote Sens Environ 135:118-129
492 Calera A, Martínez C, Melia J (2001) A procedure for obtaining green plant cover:
493 relation to NDVI in a case study for barley. Int J Remote Sens 22: 3357-3362.
494 Campos I, Neale CMU, Calera A, Balbontín C (2010) Assessing satellite-based basal
495 crop coefficients for irrigated grapes (Vitis vinífera L.). Agricultural Water
496 Management 98:45–54
497 Choudhury BJ, Idso SB, Reginato RJ (1987) Analysis of an empirical model for soil
498 heat flux under a growing wheat crop for estimating evaporation by an infrared-
499 temperature based energy balance equation. Agric For Meteorol 39:283-297
500 Cihlar J, Dobson MC, Schmugge T, Hoogeboom P, Janse ARP, Baret F, Guyot G, Le
501 Toan T, Pampaloni P (1987) Procedures for the description of agricultural crops
502 and soils in optical and microwave remote sensing studies. Int J Remote Sen
503 8:427-439
504 Colaizzi PD, Kustas WP, Anderson, MC, Agam N, Tolk JA, Evett SR, Howell TA,
505 Gowda PH, O´Shaughnessy SA (2012) Two-source energy balance model
506 estimates of evapotranspiration using component and composite surface
507 temperatures. Adv Water Res 50:134-151
508 FAO (2014) FAO Statistical Database (online). Consultation: January 20, 2014.
509 http://faostat3.fao.org/home/E
510 Farg E, Arafat SM, Abd El-Wahed MS, El-Gindy AM (2012) Estimation of
511 Evapotranspiration ETc and crop coefficient Kc of wheat, in south Nile Delta of

512 Egypt using integrated FAO-56 approach and remote sensing data. The Egyptian
513 Journal of Remote Sensing and Space Sciences 15:83-89
514 French AN, Hunsaker DJ, Clarke TR, Fitzgerald GJ, Luckett WE, Pinter PJ. Energy
515 balance estimation of evapotranspiration for wheat grown under variable
516 management practices in Central Arizona. Trans. ASABE 2007, 50(6):2059-71
517 Gao F, Kustas WP, Anderson MC (2012) A Data Mining Approach for Sharpening
518 Thermal Satellite Imagery over Land. Remote Sensing 4:3287-3319
519 Gao Y, Yang L, Shen X, Li X, Sun J, Duan A, Wu L (2014) Winter wheat with
520 subsurface drip irrigation (SDI): Crop coefficients, water-use estimates, and
521 effects of SDI on grain yield and water use efficiency. Agr Water Manage
522 146:1-10
523 Ghamarnia H, Miri E, Ghobadei M (2014) Determination of water requirement, single
524 and dual crop coefficients of black cumin (*Nigella sativa L.*) in a semi-arid
525 climate. Irr Sci 32(1):67-76
526 Gontia NK, Tiwari KN (2010) Estimation of crop coefficient and evapotranspiration of
527 wheat (triticum aestivum) in an irrigation command using remote sensing and
528 GIS. Water Resour Manage (24):1399-1414
529 Howell TA, Schneider AD, Dusek DA, Marek TH, Steiner JL. Calibration and scale
530 performance of Bushland wighing lysimeters. Trans. ASAE, 1995, 38(4):1019-
531 24
532 Howell TA, Evett SR, Tolk JA, Copeland KS, Dusek DA, Colaizzi PD (2006) Crop
533 coefficients developed at Bushland, Texas for corn, wheat, sorghum, soybean,
534 cotton, and alfalfa. In: Proceeding of the World Environmental and Water
535 Resources Congress, Omaha, NE, p. 9.

536 Howell TA, Evett SR, Tolk JA, Copelan KS, Marek TH (2012) Evapotranspiration and
537 crop coefficients for irrigated sunflower in the Southern High Plains. ASABE
538 Paper No. 12-1338306. St. Joseph, Mich.: ASABE
539 Hunsaker DJ, Pinter Jr PJ, Kimball BA (2005) Wheat basal crop coefficients
540 determined by normalized difference vegetation index Irri Sci 24(1):1-14
541 Kjaersgaard JH, Plauborg FL, Mollerup M, Petersen CT, S. Hansen (2008) Crop
542 Coefficients for winter wheat in a sub-humid climate regime. Agric Water
543 Manag 95:918-924
544 Kustas WP, Alfieri JG, Anderson MC, Colaizzi PD, Prueger JH, Evett SR, Neale CMU,
545 French, AN, Hipps LE, Chávez JL, Copeland KS, Howell TA (2012) Evaluating
546 the two-source energy balance model using local thermal and surface flux
547 observations in a strongly advective irrigated agricultural area. Adv Water Res
548 50:120-133
549 Li F, Kustas WP, Prueger JH, Diak GR (2005) Utility of remote sensing based two-
550 source energy balance model under low and high vegetation cover conditions. J
551 Hydromet 6:878-91
552 López-Urrea R, Martín de Santa Olalla F, Fabeiro C, Moratalla A (2006) Testing
553 evapotranspiration equations using lysimeter observations in a semiarid climate.
554 Agr Water Manage 85:15–26
555 López-Urrea, R, Montoro A, González-Piqueras J, López-Fuster P, and Fereres E
556 (2009) Water use of spring wheat to raise water productivity. Agr Water Manage
557 96:1305–1310
558 López-Urrea R, Montoro A, Mañas F, López-Fuster P, Fereres E (2012)
559 Evapotranspiration and Crop Coefficients from Lysimeter Measurements of
560 mature ‘Tempranillo’ wine grapes. Agric Water Manage 112:13-20

López-Urrea R, Montoro A, Trout TJ (2014) Consumptive Water Use and Crop Coefficients of Irrigated Sunflower. Irrig Sci 32(2): 99-109

MAGRAMA (2014) Anuario de Estadística 2013. Ministerio de Agricultura, Alimentación y Medio Ambiente. Madrid. pp. 1095.

Norman JM, Kustas WP, Humes KS (1995) A two-source approach for estimating soil and vegetation energy fluxes from observations of directional radiometric surface temperature. Agric For Meteorol 77:263-293.

Priestley CHB, Taylor RJ (1972) On the assessment of surface heat flux and evaporation using large-scale parameters. Mon Weather Rev 100:81-92.

Rubio E, Caselles V, Coll C, Valor E, Sospedra F (2003) Thermal-infrared emissivities of natural surfaces: improvements on the experimental set-up and new measurements. Int J Remote Sens 24:5379-5390

Sadras VO, Rodriguez D (2010) Modelling the nitrogen-driven tradeoff between nitrogen utilisation efficiency and water use efficiency of wheat in eastern Australia. Field Crops Res. 118:297–305

Sánchez JM, Kustas WP, Caselles V, Anderson M (2008) Modelling surface energy fluxes over maize using a two-source patch model and radiometric soil and canopy temperature observations. Remote Sens Environ 112:1130-1143

Sánchez JM, López-Urrea R, Rubio E, Caselles V (2011) Determining water use of sorghum from two-source energy balance and radiometric temperatures. Hydrol Earth Syst Sc 15:3061-3070

Sánchez JM, López-Urrea R, Rubio E, González-Piqueras J, Caselles V (2014) Assessing crop coefficients of sunflower and canola using two-source energy balance and thermal radiometry. Agr Water Manage 137:23-29

585 Shahrokhnia MH, Sepaskhah AR (2013) Single and dual crop coefficient and crop
586 evapotranspiration for wheat and maize in a semi-arid region. Theor Appl
587 Climatol, 114:495-510
588 Sun HY, Liu CM, Zhang XY, Shen YJ, Zhang YQ (2006) Effects of irrigation on water
589 balance, yield and WUE of winter wheat in the North China Plain. Agric Water
590 Manag 85:211–218
591 Williams LE, Ayars JE (2005) Grapevine water use and the crop coefficient are linear
592 functions of the shaded area measured beneath the canopy. Agricultural and
593 Forest Meteorology 132:201–211:
594 Willmott CJ (1982) Some comments on the evaluation of model performance. Bulletin
595 American Meteorological Society 63(11):1309-1313
596 Yang G, Pu R, Zhao Ch, Xue X (2014) Estimating high spatiotemporal resolution
597 evapotranspiration over a winter wheat field using an IKONOS image based
598 complementary relationship and Lysimeter observations. Agr Water Manage
599 133:34-43
600 Zhang B, Liu Y, Xu D, Zhao N, Lei B, Rosa RD, Paredes P, Paço TA, Pereira LS
601 (2013) The dual crop coefficient approach to estimate and partitioning
602 evapotranspiration of the winter wheat-summer maize crop sequence in North
603 China Plain. Irrig Sci 31:1303-1316
604 Zhang S, Zhao H, Lei H, Shao H, Liu T (2015) Winter wheat productivity evaluated by
605 the developed remote sensing evapotranspiration model in Hebei Plain, China.
606 The Scientific World Journal, article ID 384086.
607 Zhao N, Liu Y, Cai J, Paredes P, Rosa RD, Pereira LS (2013) Dual crop coefficient
608 modelling applied to the winter wheat-summer maize crop sequence in North

China Plain: Basal crop coefficients and soil evaporation component. Agr Water Manage 117:93-105

Table 1. Mean values of the meteorological variables: air temperature (T_a), relative humidity (H_r), wind speed (u), solar irradiance (S), reference evapotranspiration (ET_0), soil moisture at -10 cm (SM), and cumulated precipitation (Prec.) and irrigation (Irr.), at the wheat plot for the entire experiment.

	T_a (ºC)	H_r (%)	u (m s^{-1})	S (W m^{-2})	SM ($m^3 m^{-3}$)	Prec. (mm)	Irr. (mm)	ET_0 (mm d^{-1})
February*	7.3	60	4.2	134	0.28	8	16	1.9
March	8.8	66	3.9	196	0.28	2	70	2.9
April	13.8	69	3.0	255	0.27	37	46	4.2
May	15.9	60	2.6	302	0.28	5	183	5.3
June	20.1	59	2.4	305	0.25	43	119	5.6

* Starting 12 February.

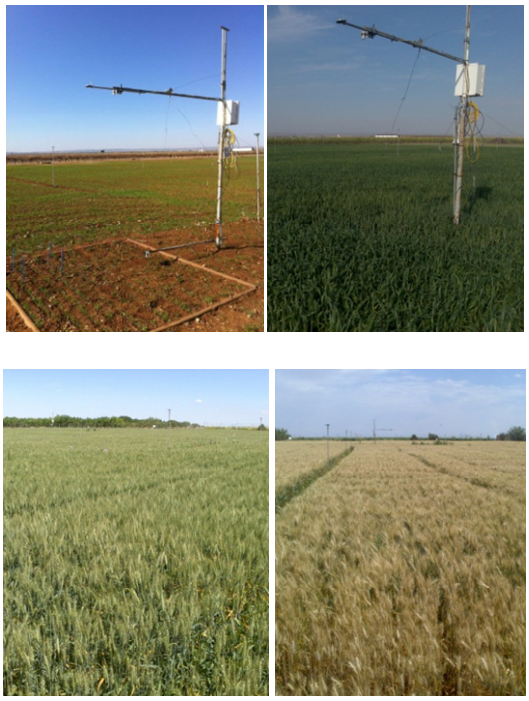

620

621 **Fig. 1** Experimental setup over the lysimeter for DOYs 55 and 129 (top), and view of

622 the wheat field conditions for DOYs 153 and 174 (bottom)

623

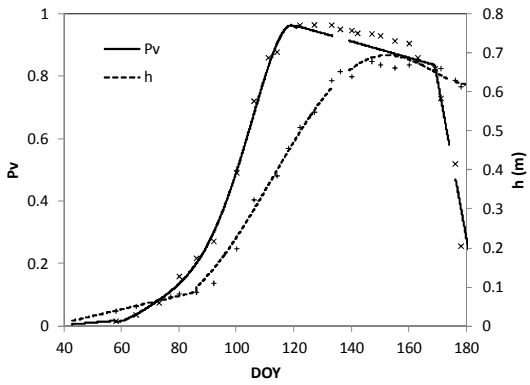

624

625 **Fig. 2** The 2014 wheat season phenology showing fractional vegetation cover (P_v) and

626 the canopy height (h). Marks correspond to measured values and lines represent

627 modeled behavior

628

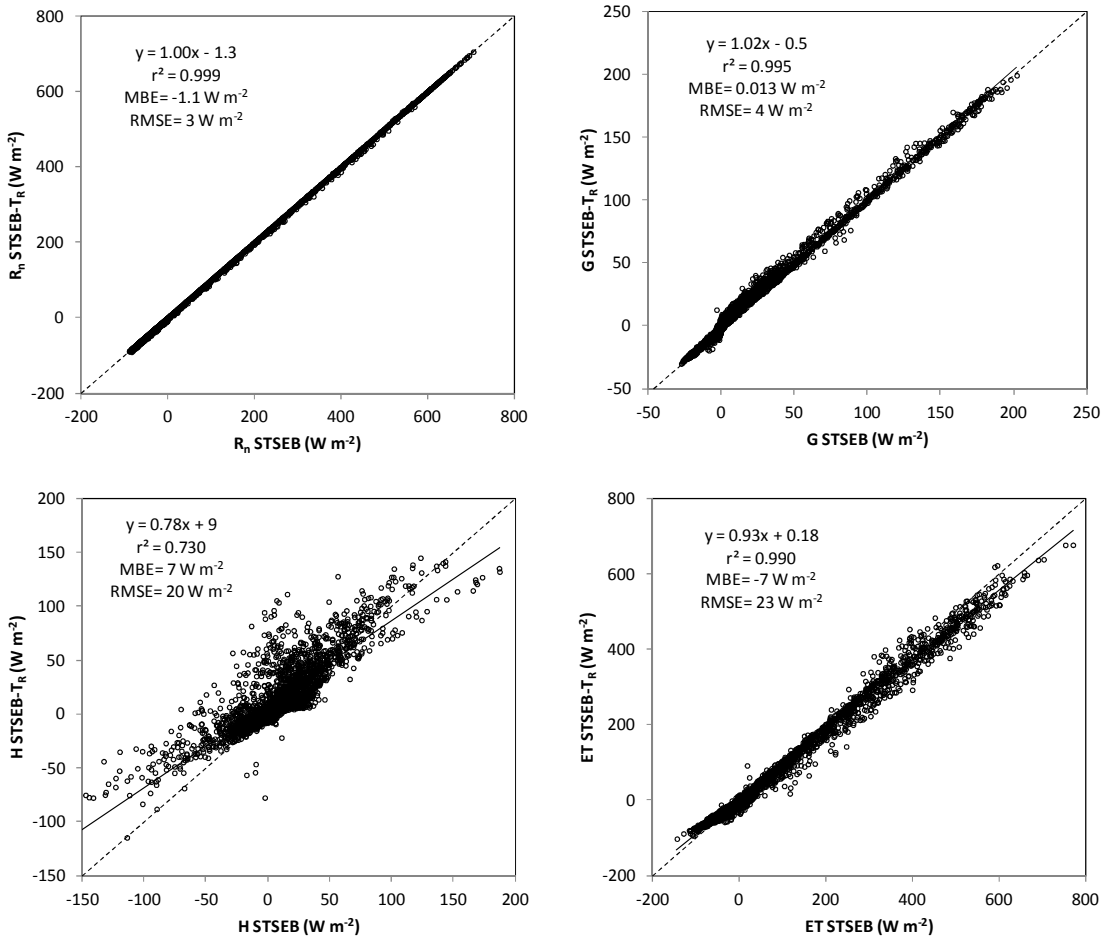

629

630 **Fig. 3** Comparison of hourly estimates of the different terms of the surface energy
631 balance (R_n, G, H, and ET), using the original STSEB approach and the modified
632 STSEB-T_R formulation.

633

634

635

636

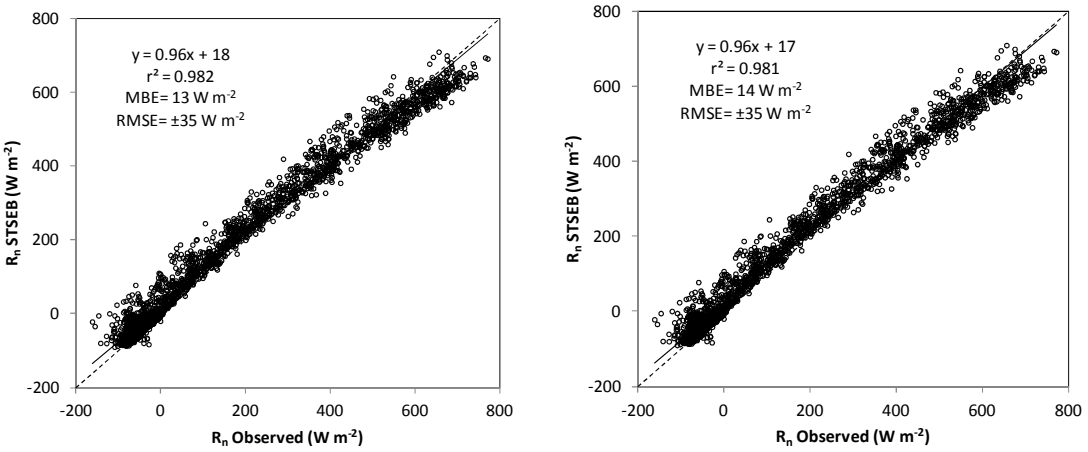

(a)

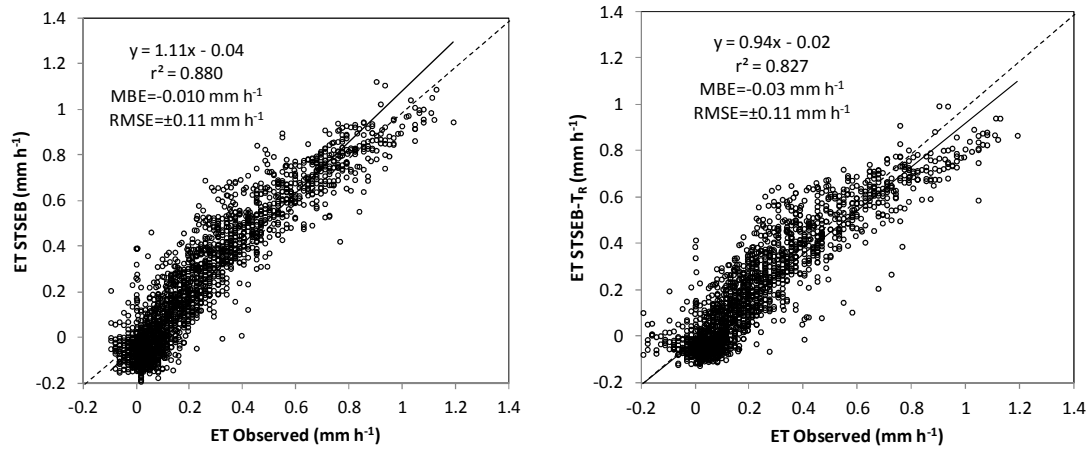

(b)

Fig. 4 Calculated vs. ground-measured hourly variables using the original STSEB approach and the modified STSEB-T_R formulation: (a) net radiation, (b) evapotranspiration

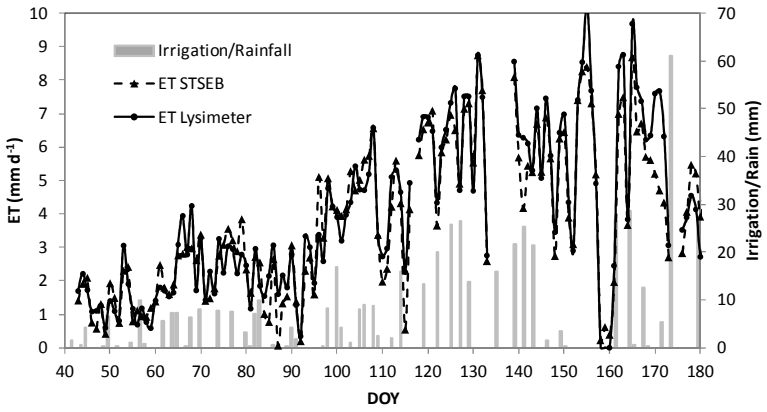

(a)

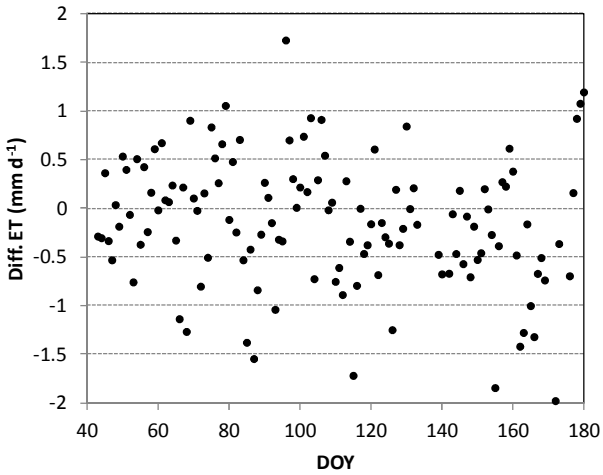

(b)

Fig. 5 (a) Evolution of modeled and observed daily ET values for the wheat season. Irrigation and rainfall amounts are also included. (b) Daily ET discrepancy (modeled ET- observed ET) over the growing season

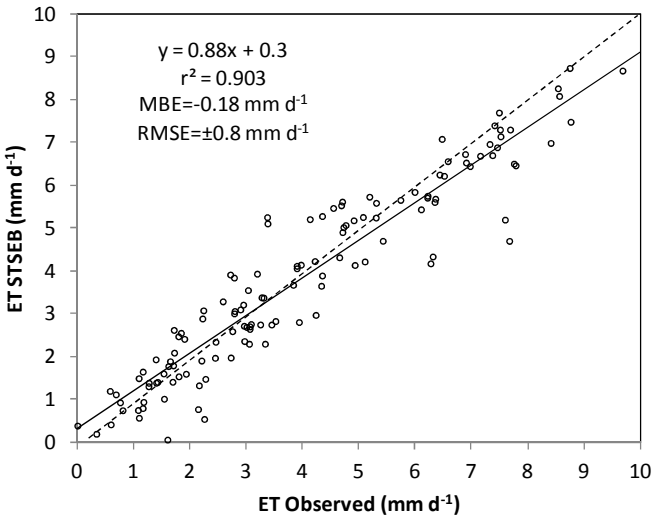

Fig. 6 Comparison of daily ET estimates with lysimeter measurements

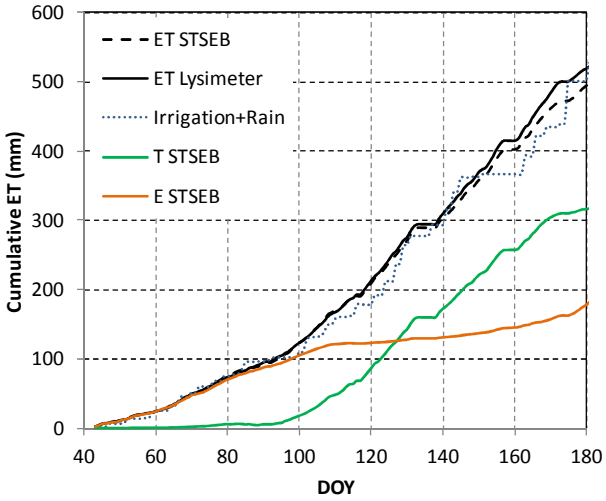

Fig. 7 Cumulative values of predicted ET, E, and T values, for the whole wheat season, together with observed ET and irrigation+rain amount

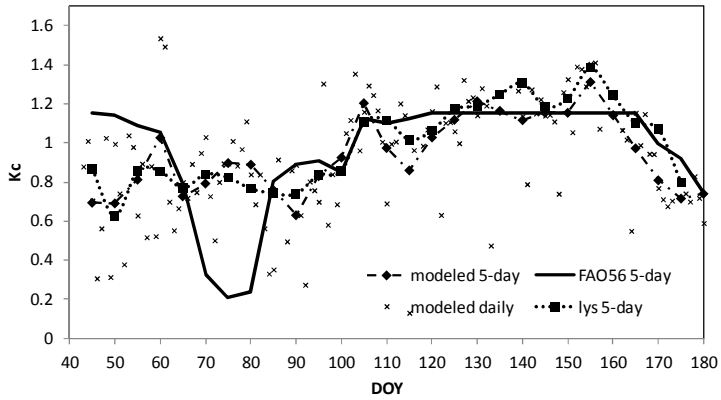

667
668 (a)

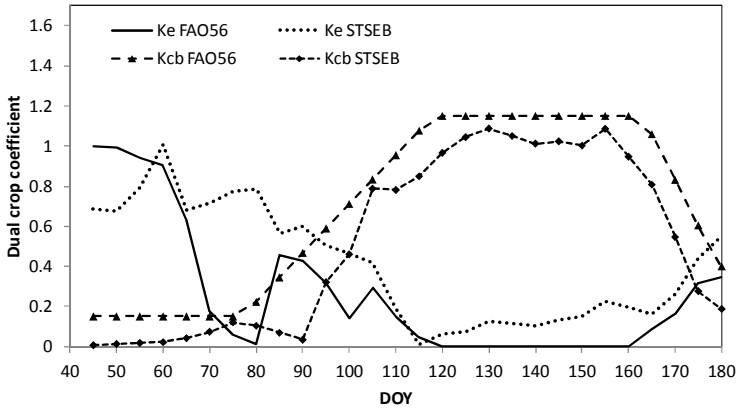

669
670 (b)

671 **Fig. 8** Comparison of modeled values of crop coefficients with those calculated from
672 lysimeter measurements and proposed by FAO56: (a) K_c, (b) K_e and K_{cb}

673
674
675
676